THE ASTROPHYSICAL JOURNAL, 465:L119–L122, 1996 July 10

PROBING THE ECLIPSE REGION OF A BINARY MILLISECOND PULSAR

B. W. STAPPERS,[1] M. BAILES,[2,3] A. G. LYNE,[4] R. N. MANCHESTER,[2] N. D'AMICO,[5,6]
T. M. TAURIS,[7] D. R. LORIMER,[4,8] S. JOHNSTON,[9] AND J. S. SANDHU[10]
Received 1996 March 13; accepted 1996 April 29

ABSTRACT

We report the discovery of a new eclipsing millisecond binary pulsar system, PSR J2051−0827. The pulsar has a period of 4.5 ms and is in a very compact circular orbit with a companion of mass $\sim 0.03\ M_\odot$. Observations at low frequencies show that the eclipse duration is approximately 10% of the orbital period. However, at high radio frequencies, pulses are often detected throughout the eclipse region, revealing interesting time-variable density structure in the eclipsing plasma.

Subject headings: binaries: eclipsing — pulsars: individual (PSR J2051−0827)

1. INTRODUCTION

It has been proposed that isolated millisecond pulsars are formed from binary systems where the strength of the pulsar radiation is able to evaporate the binary companion (Alpar et al. 1982; Rasio, Shapiro, & Teukolsky 1989; Bhattacharya & van den Heuvel 1991). The discovery of the "black widow" pulsar B1957+20 (Fruchter, Stinebring, & Taylor 1988) lent weight to this idea. However, whether the companion in this system will eventually be evaporated is not clear. Observations of the pulse times of arrival near the eclipse boundaries (Fruchter et al. 1990; Ryba & Taylor 1991) and the lack of eclipse in the 20 cm continuum flux (Fruchter & Goss 1992) indicate that the electron column density in the eclipse medium is low and hence suggest low mass-loss rates. If the companion radius is close to its Roche lobe, then this will facilitate the mass loss. A companion radius close to the Roche limit is also required by models of the companion's light curve (Callanan, van Paradijs, & Regelink 1995) and the tidal activity proposed to explain the variable orbital period derivative (Applegate & Shaham 1994).

Eclipsing binary pulsars also provide excellent tools with which to study the relativistic wind emanating from pulsars. Interactions of this wind with the wind from the companion star modify the eclipse properties. However, the eclipse mechanism in the known eclipsing systems is still very uncertain (Thompson et al. 1994 and references therein).

We have discovered a new eclipsing binary millisecond pulsar and have carried out timing observations at a number of frequencies. These data indicate that this system is at a similar evolutionary epoch to PSR B1957+20 and thus provides an additional test of the standard formation model for isolated millisecond pulsars. The detection of time-variable structure in the distribution of electrons in the eclipse region will allow further constraints to be placed on any eclipse mechanisms in similar systems.

2. OBSERVATIONS AND ANALYSIS

PSR J2051−0827 was discovered with the Australia Telescope National Facility's Parkes 64 m radio telescope in a 436 MHz survey of the entire southern sky (Bailes et al. 1994; Manchester et al. 1996). At the dispersion measure (DM) and period of the pulsar (20.7 cm^{-3} pc and 4.5 ms, respectively) the survey was sensitive to pulsars with a mean flux density greater than 5 mJy. The pulsar was discovered in data taken on 1994 May 13, and follow-up observations soon revealed that the pulsar was a member of a short-period binary system with a circular orbit.

Regular timing observations have been made since the discovery with the Parkes telescope and the 76 m Lovell radio telescope at Jodrell Bank at frequencies between 408 MHz and 2.0 GHz; dual-polarization, cryogenic receivers were used at both observatories. The filter-bank timing systems used are similar to those described in detail elsewhere (Bailes et al. 1994; Bell et al. 1995). The 660 MHz data used in Figure 1 were obtained using the Caltech correlator pulsar timing machine (Navarro 1994) at Parkes. This allows high time resolution observations by synthesizing up to 256 frequency channels in 32 MHz total bandwidth in each polarization and sampling at 4.5 μs. Pulse times of arrival (TOAs) were determined by fitting a standard pulse template to observed profiles and analyzed using the TEMPO (Taylor & Weisberg 1989) program, together with the DE200 ephemeris of the Jet Propulsion Laboratory (Standish 1982) and a simple Keplerian model of a binary system (Blandford & Teukolsky 1976).

Timing parameters for the PSR J2051−0827 system are given in Table 1; the errors shown in parentheses are twice the formal TEMPO errors. This best-fitting model was obtained by setting the eccentricity and longitude of periastron to zero, and excluding all data between binary phases 0.1 and 0.4 to avoid delays associated with the atmosphere of the companion

[1] Mount Stromlo and Siding Spring Observatories, Institute of Advanced Studies, Australian National University, Private Bag, Weston Creek, ACT 2611, Australia.
[2] Australia Telescope National Facility, CSIRO, P.O. Box 76, Epping, NSW 2121, Australia.
[3] Physics Department, University of Melbourne, Parkville, Vic 3052, Australia.
[4] University of Manchester, NRAL, Jodrell Bank, Macclesfield, Cheshire SK11 9DL, UK.
[5] Osservatorio Astronomico di Bologna, via Zamboni 33, 40126 Bologna, Italy.
[6] Istituto di Radioastronomia del CNR, via Gobetti 101, 40129 Bologna, Italy.
[7] Institute of Physics and Astronomy, Aarhus University, DK-8000 Aarhus C, Denmark; and Australia Telescope National Facility, CSIRO, P.O. Box 76, Epping, NSW 2121, Australia.
[8] Max-Planck-Institut für Radioastronomie, Auf dem Hügel 69, D-53121 Bonn, Germany.
[9] Research Centre for Theoretical Astrophysics, University of Sydney, NSW 2006, Australia.
[10] California Institute of Technology, MS 105-24, Pasadena, CA 91125

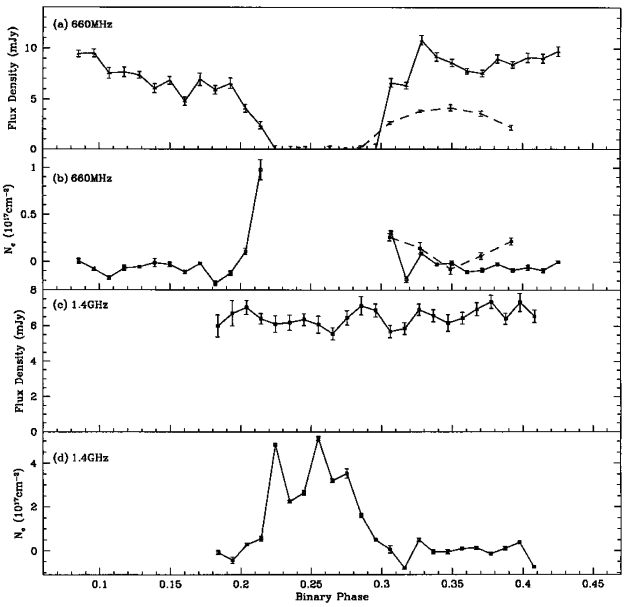

FIG. 1.—Eclipse characteristics of PSR J2051−0827 at 660 MHz and 1.4 GHz are shown as a function of orbital phase. The observations were made on 1995 October 1 (660 MHz, *solid line*), October 2 (660 MHz, *dashed line*), and October 3 (1.4 GHz). Each data point corresponds to a 90 s integration. (*a*) Flux density variation at 660 MHz. Note the gradual decrease in the pulse amplitude during ingress and the rapid return to full pulse strength at egress. (*b*) Electron column density variations, also at 660 MHz, determined from excess time delays. (*c*) Flux density for a 1.4 GHz observation where pulses were detected throughout the eclipse region. (*d*) The corresponding electron column density.

star, which are expected to be maximum close to the eclipse. The 2.38 hr orbital period of this system is the second shortest pulsar orbital period known, behind PSR B1744−24A (Lyne et al. 1990), and the shortest for pulsar binaries outside globular clusters. At 436 MHz the mean flux density of the pulsed radiation away from the eclipse is ∼22 mJy, and at 1.4 GHz it is ∼5 mJy, giving a spectral index $\alpha \sim -1.2$, where $S \propto \nu^{\alpha}$ is the flux density and ν is the observing frequency. The pulse profile appears rather simple in shape and has a width at half-power of ∼10% of the pulse period.

The dispersion-derived distance (Taylor & Cordes 1993) to the pulsar, $d = 1.3$ kpc, is relatively small. Consequently, there may be a significant contribution to the measured value of $\dot{P}$ from the Shklovskii effect (Shklovskii 1970; Camilo, Thorsett, & Kulkarni 1994), in which the transverse velocity v_t of a pulsar increases the intrinsic $\dot{P}$ by an amount Pv_t^2/cd, where c is the velocity of light. The transverse velocity of PSR J2051−0827 is unlikely to exceed 100 km s^{-1} if this pulsar is similar to other millisecond pulsars (Nicastro & Johnston 1995; Nice & Taylor 1995). In that event, the contribution to $\dot{P}$ is 0.4×10^{-20}, or about 30% of the measured value. In view of this, the characteristic age 5×10^9 yr and surface magnetic field strength 2.4×10^8 G should be taken as preliminary.

TABLE 1

PARAMETERS FOR PSR J2051−0827

Parameter	Value
Right ascension (J2000)	$20^h51^m07\overset{s}{.}5118(10)$
Declination (J2000)	−08°27′37″.78(4)
Epoch of period (MJD)	49530.0
Period (s)	0.00450864174335(2)
Period derivative ($\times 10^{-20}$)	1.3(1)
Dispersion measure (cm^{-3} pc)	20.741(8)
Orbital period (days)	0.099110266(4)
Orbital period derivative, $\lvert\dot{P}_b\rvert$	$\leq 25 \times 10^{-12}$
Projected semimajor axis (lt-s)	0.045086(10)
Eccentricity	$< 3 \times 10^{-4}$
Epoch of ascending node (MJD)	49642.173031(4)
Root mean square timing residual (μs)	31
Galactic longitude	$39\overset{\circ}{.}19$
Galactic latitude	$-30\overset{\circ}{.}41$
Mass function ($M_\odot$)	1.0010×10^{-5}
Minimum companion mass ($M_\odot$)	0.027

The mass function $f(m_p, m_c)$ relates the orbital period, P_b, and the projected semimajor axis of the pulsar, $a_p \sin i$, where i is the orbital inclination, to the mass of the pulsar, m_p, and of the companion, m_c:

$$f(m_p, m_c) = \frac{(m_c \sin i)^3}{(m_p + m_c)^2} = \frac{4\pi^2}{G}\frac{(a_p \sin i)^3}{P_b^2} = (1.0010 \pm 0.0003) \times 10^{-5}\, M_\odot . \quad (1)$$

Assuming a pulsar mass $m_p = 1.4\ M_\odot$, the minimum companion mass m_c is $0.027\ M_\odot$. The existence of eclipses implies that $i \gtrsim 60°$ and hence that the companion mass is within a factor of 1.2 of the minimum. This system is extremely compact with a separation of the binary components $a = (a_p + a_c) \approx 1.0\ R_\odot$, approximately independent of the actual value of i.

3. ECLIPSE CHARACTERISTICS

The duration of the eclipse at 436 MHz is ∼10% of the orbital period, which implies a radius for the eclipse region surrounding the companion $r_{\rm eclip} \approx 2 \times 10^8$ m $\approx 0.3\ R_\odot$. The radius of the Roche lobe (Eggleton 1983) of the companion is, for $60° < i < 90°$,

$$R_L = \frac{0.49aq^{2/3}}{0.6q^{2/3} + \ln(1 + q^{1/3})} \sim 0.13\ R_\odot , \quad (2)$$

where $q = m_c/m_p$ is the mass ratio. Thus the eclipse material extends well beyond the maximum radius at which it remains gravitationally bound to the companion. As for PSR B1744−24A (Lyne et al. 1990), PSR B1718−19 (Lyne et al. 1993), and PSR B1957+20 (Fruchter et al. 1988), there must be some source which is constantly replenishing the eclipse material. Such mass loss would be more likely for a companion with a radius which is close to that of the Roche lobe.

The radius of a degenerate dwarf star can be estimated from the mass-radius relation of Shapiro & Teukolsky (1983). A hydrogen-rich ($X \approx 0.7$) white dwarf with $m_c \sim 0.027\ M_\odot$ has $r_c = 0.10\ R_\odot$, whereas a helium dwarf ($X = 0.0$) with the same mass has $r_c = 0.04\ R_\odot$.

However, if the companion is nondegenerate and the impinging energy flux density from the pulsar is greater than $\sim 10^{10}$–10^{11} ergs s^{-1} cm^{-2}, then the radius of the companion may increase considerably because of a change in the ionization state of its envelope (Podsiadlowski 1991). The spin-down power of PSR J2051−0827 is $\dot{E} \approx -6 \times 10^{33}$ ergs s^{-1}, and the energy flux at the companion's surface is $\sim 10^{11}$ ergs s^{-1} cm^{-2} if the pulsar radiation is isotropic, making a bloated companion and Roche lobe overflow a distinct possibility.

High signal-to-noise ratio eclipse data at 660 MHz are shown in the top two panels of Figure 1. The eclipse duration

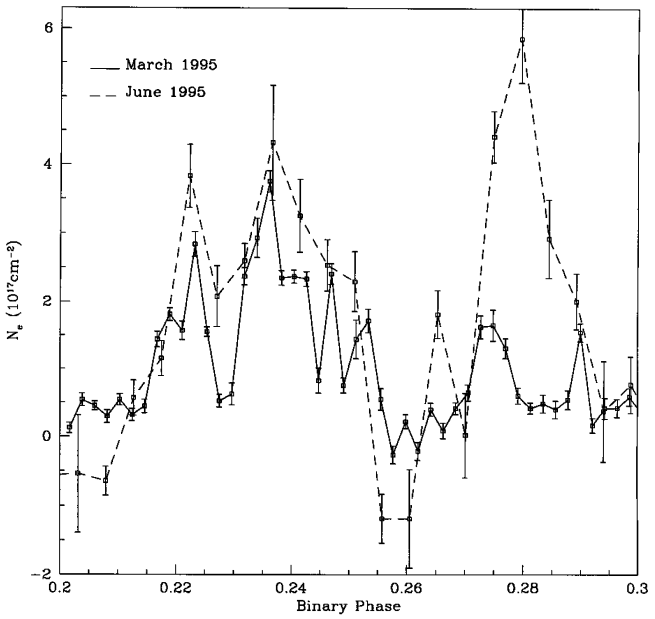

FIG. 2.—Electron density variation at 2.0 GHz, measured in observations on 1995 March 13 and June 19, show that there are both structure and variability in the eclipse region.

of PSR J2051−0827 at low frequencies, seen in Figure 1*a*, is a similar fraction of the orbital period to that of PSR B1957+20. The change in the electron column density (or DM) in the path of the pulsar, obtained from the excess delays relative to the orbital model given in Table 1, is shown in Figure 1*b*. As eclipse is approached, the pulse decreases in amplitude but does not change in shape, showing that the eclipse mechanism removes photons from the line of sight but does not significantly scatter the pulse. Thus either absorption or large-angle scattering may be responsible.

A number of observations were made at 1.4 GHz between phases 0.1 and 0.4, and the pulsar was detected throughout the low-frequency eclipse region in approximately half of them. An example where there was little or no decrease in pulsed flux density is shown in Figures 1*c* and 1*d*. The rise to the first peak in the electron density corresponds to the phase at the low-frequency eclipse ingress; there is no evidence for extended delay at egress. These observations indicate structure in the density of the eclipsing gas.

Observations at 2.0 GHz made on 1995 March 13 and 1995 June 19, when the pulsar was bright, possibly amplified by interstellar scintillation, have allowed us to probe the eclipse region with a significantly improved time resolution of 18 s and 40 s in the two sessions. The electron column density implied by the TOA delays at these two epochs is shown in Figure 2. While there is enhancement between phases 0.21 and 0.29, as in Figure 1*d*, the detailed structure is different on each occasion, showing that the eclipsing plasma is highly variable.

The variation in eclipse duration between 436 and 660 MHz seems to be frequency dependent, with $\Delta t \propto \nu^{\beta}$ and $\beta \sim -0.15$, although scarcity of data points and the substantial integration time required for pulse detection at the limits of the eclipse region make it difficult to place strong limits on the frequency dependence. While we cannot rule out refractive eclipses based on the frequency dependence of the eclipse, the very low electron column density at ingress and egress is much less than that required by this mechanism (Thompson et al. 1994; Rasio, Shapiro, & Teukolsky 1991).

The maximum delay in pulse arrival times at 436 MHz, just before eclipse, gives $N_e \sim 3 \times 10^{16}$ cm^{-2}. If the eclipses at 436 MHz result from free-free absorption (Thompson et al. 1994), and assuming the eclipse region is a sphere of radius $r = r_{\rm eclip}$, then the gas temperature is $T \lesssim 10^3 f_{\rm cl}^{2/3}$ K, where $f_{\rm cl} = \langle n_e^2 \rangle / \langle n_e \rangle^2$ is the clumping factor and n_e is the electron density. At 660 MHz we probe deeper into the eclipse region, and the electron column density is $N_e \sim 10^{17}$ cm^{-2} at the eclipse boundary. The gas temperature required for free-free absorption is then $T \lesssim 3 \times 10^3 f_{\rm cl}^{2/3}$ K. These results suggest that, if the low-frequency eclipses in this system are caused by free-free absorption, the material lost from the companion must be either very cold or highly clumped.

The highly variable nature of the eclipse duration and the electron density structure in the eclipsing region indicate that we are probing a wind zone where there is substantial motion of the eclipse material.

4. DISCUSSION

So what is the ultimate fate of PSR J2051−0827? The mass-loss rate can be estimated by setting the momentum flux of the wind equal to that of the pulsar spin-down (Thompson et al. 1994). For PSR J2051−0827, if we assume a mean free electron density of 10^7 cm^3 in the eclipse region, the mass-loss rate is only $\sim 10^{-14}$ $M_\odot$ yr^{-1}, far less than is required to evaporate the companion completely on any reasonable timescale. When the original eclipsing millisecond pulsar was first discovered, it appeared that we might have been lucky enough to find the short-lived "missing link" between low-mass X-ray binaries and solitary millisecond pulsars. However, millisecond pulsars are thought to have active lifetimes of $\sim 10^{10}$ yr, and there are two eclipsing pulsars and only eight solitary millisecond pulsars known in the Galactic disk. Although we are still dealing with small-number statistics, it appears that both birthrate and mass-loss estimates suggest that in some systems the eclipse phase can last for billions of years.

We thank J. F. Bell for helpful discussions. B. W. S. received support from an ANU Ph.D. scholarship and the ATNF student program.

REFERENCES

Alpar, M. A., Cheng, A. F., Ruderman, M. A., & Shaham, J. 1982, Nature, 300, 728
Applegate, J. H., & Shaham, J. 1994, ApJ, 436, 312
Bailes, M., et al. 1994, ApJ, 425, L41
Bell, J. F., Bailes, M., Manchester, R. N., Weisberg, J. M., & Lyne, A. G. 1995, ApJ, 440, L81
Bhattacharya, D., & van den Heuvel, E. P. J. 1991, Phys. Rep., 203, 1
Blandford, R., & Teukolsky, S. A. 1976, ApJ, 205, 580
Callanan, P. J., van Paradijs, J., & Regelink, R. 1995, ApJ, 439, 928
Camilo, F., Thorsett, S. E., & Kulkarni, S. R. 1994, ApJ, 421, L15
Eggleton, P. P. 1983, ApJ, 268, 368
Fruchter, A. S., et al. 1990, ApJ, 351, 642
Fruchter, A. S., & Goss, W. M. 1992, ApJ, 384, L47
Fruchter, A. S., Stinebring, D. R., & Taylor, J. H. 1988, Nature, 333, 237
Lyne, A. G., Biggs, J. D., Harrison, P. A., & Bailes, M. 1993, Nature, 361, 47
Lyne, A. G., et al. 1990, Nature, 347, 650
Manchester, R. N., et al. 1996, MNRAS, in press
Navarro, J. 1994, Ph.D. thesis, California Inst. Technol.
Nicastro, L., & Johnston, S. 1995, MNRAS, 273, 122
Nice, D. J., & Taylor, J. H. 1995, ApJ, 441, 429

Podsiadlowski, P. 1991, Nature, 350, 136
Rasio, F. A., Shapiro, S. L., & Teukolsky, S. A. 1989, ApJ, 342, 934
———. 1991, A&A, 241, L25
Ryba, M. F., & Taylor, J. H. 1991, ApJ, 380, 557
Shapiro, S. L., & Teukolsky, S. A. 1983, Black Holes, White Dwarfs, and Neutron Stars: The Physics of Compact Objects (New York: Wiley-Interscience)
Shklovskii, I. S. 1970, Soviet Astron., 13, 562
Standish, E. M. 1982, A&A, 114, 297
Taylor, J. H., & Cordes, J. M. 1993, ApJ, 411, 674
Taylor, J. H., & Weisberg, J. M. 1989, ApJ, 345, 434
Thompson, C., Blandford, R. D., Evans, C. R., & Phinney, E. S. 1994, ApJ, 422, 304